Surface plasmon interference excited by tightly focused laser beams

A. Bouhelier,[1,*] F. Ignatovich,[2] A. Bruyant,[1,4] C. Huang,[1] G. Colas des Francs,[1] J.-C. Weeber,[1] A. Dereux,[1] G. P. Wiederrecht,[3] and L. Novotny[2]

[1]*Institut Carnot de Bourgogne, CNRS-UMR 5209, Université de Bourgogne, 21078 Dijon, France*
[2]*The Institute of Optics, University of Rochester, Rochester, New York 14627, USA*
[3]*Center for Nanoscale Materials, Argonne National Laboratory, Argonne, Illinois 60439, USA*
[4]*Present address: Laboratoire de Nanotechnologie et d'Instrumentation Optique, Université Technologique de Troyes, France*
[*]*Corresponding author: alexandre.bouhelier@u-bourgogne.fr*

Received May 2, 2007; revised July 23, 2007; accepted July 23, 2007;
posted August 1, 2007 (Doc. ID 82525); published August 20, 2007

We show that interfering surface plasmon polaritons can be excited with a focused laser beam at normal incidence to a plane metal film. No protrusions or holes are needed in this excitation scheme. Depending on the axial position of the focus, the intensity distribution on the metal surface is either dominated by interferences between counterpropagating plasmons or by a two-lobe pattern characteristic of localized surface plasmon excitation. Our experiments can be accurately explained by use of the angular spectrum representation and provide a simple means for locally exciting standing surface plasmon polaritons. © 2007 Optical Society of America

OCIS codes: 240.6680, 180.5810, 310.6860.

Because surface plasmon polaritons (SPPs) can be spatially localized to dimensions significantly smaller than the wavelength of free-propagating radiation, they are of potential interest for various applications such as nanoscale waveguides [1,2], optical antennas [3], sensors [4], negative refraction [5], high-resolution microscopy [6], and nonlinear optics [7]. The coherent excitation of SPPs in metal films of complex permittivity $\tilde{\epsilon}_m(\omega)$ is governed by a dispersion law that imposes a relatively narrow set of resonant in-plane wave vectors k_{sp} at a given excitation frequency ω. Localized optical fields largely satisfy this dispersion relation because they intrinsically contain a large spectrum of in-plane wave vectors. The electromagnetic field scattered by near-field apertures [8,9], or by nanometer-sized defects on the metal surface such as protrusions [10,11] and holes [12–14] can couple their SPP resonant wave vectors and locally launch propagating SPPs. Due to the very nature of such excitation, localized fields can act as SPP point sources and are of interest for investigating and designing novel plasmonic materials and devices because they can be precisely controlled spatially and spectrally.

In this Letter, we report on the propagation of SPPs in an Ag film excited by localized fields originating from the tight focalization of a laser beam. A diffraction-limited focal spot is achieved by use of a large numerical aperture objective (N.A. >1). For oil-immersion lenses, the spread of incidence angles emanating from the reference sphere of the lens and converging towards the focus include the resonant angles responsible for SPP excitation at a metal/air interface over the complete visible range [15]. As illustrated in Fig. 1(a), the plane waves emanating from the reference sphere converge towards the geometric focus and give rise to a diffraction-limited spot containing a large spectrum of wave vectors limited by the N.A. of the lens. Qualitatively, the excitation of SPPs acts as a spatial filter by selecting two sets of diametrically opposed plane waves at incident angles $\theta = \pm\theta_{sp}$ fulfilling the SPP dispersion law [16]. The SPP waves corresponding to $+k_{sp}$ and $-k_{sp}$ are excited everywhere due to the very nature of the plane waves. A standing wave should dominate the SPP intensity distribution as a result of the interference between two counterpropagating SPP waves. Evidence for such SPP interference was recently provided by recording the fluorescence from single fluorophores deposited on a thin gold film scanned through a tightly focused laser beam [17].

In this Letter, we perform a direct measurement of the surface plasmon field and show that the SPP intensity distribution can be either dominated by interference fringes or left unmodulated, depending on the vertical position z_o of the laser focus relative to the

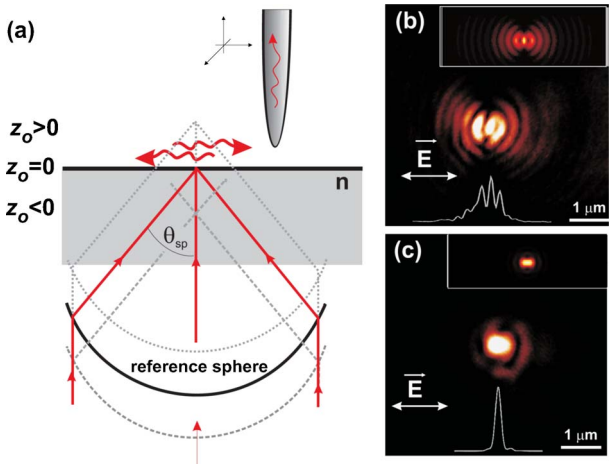

Fig. 1. (Color online) (a) Schematic of the experiment for three different focal positions z_o. (b) and (c) Intensity maps of the focal region for an Ag/air interface and a glass/air interface with cross-sectional cuts taken through the focus. Insets: calculated maps.

0146-9592/07/172535-3/$15.00

metal film. Notice that the excitation of surface plasmons with a focused laser beam can be quite different from the situation where SPPs are locally excited by a point defect or a near-field aperture. In these experiments, the SPP intensity distribution I_{spp} is *not* modulated and follows the asymptotic expression $I_{spp}(\rho,\phi)=(1/\rho)\exp(-\rho/L_{sp})\cos^2\phi$, where ρ is the distance taken from the origin of excitation, ϕ is the angle with respect to the polarization direction, and L_{sp} is the SPP propagation length [8,9,11].

In our experiment, we excite surface plasmons on a 50 nm thick silver with a tightly focused, linearly polarized Gaussian laser beam with wavelength $\lambda=632$ nm. The oil-immersion objective lens used in the experiment has an N.A. of 1.4, corresponding to an angle spread of $2\times 69°$, well beyond the SPP resonant angles $\theta_{sp}\sim\pm 48°$ for $\lambda=632$ nm. We use a strong overfilling of the back aperture, corresponding to a filling factor of $f_o\approx 2$. Aperture-type scanning near-field optical microscopy (aperture $\approx$100 nm) operated in collection mode is used to record maps of the surface plasmon intensity [18,19].

Figure 1(b) shows an image of the light collected by the probe scanned laterally through the focal region. The polarization of the incident electric field was aligned horizontally as indicated by the arrow and is kept the same throughout this Letter. A cross-sectional cut through the focus shows a modulation of the intensity that extends well beyond the center of the focus. To compare the experimental image with calculated intensity distributions we use the full angular spectrum representation, which decomposes the incident radiation into plane waves and takes into account multiple reflections between the glass/metal/air interfaces. The vertical component of the electric field on the metal film is calculated as [20]

$$E_z(\rho,\phi)\propto\cos\phi\int_0^{NA} ds\,\exp[ik_o z_o(n^2-s^2)^{1/2}]\times\exp[-(s/NAf_o)^2]\frac{s^2t^p(s)}{[n^2-s^2]^{1/4}}J_1(sk_o\rho). \quad (1)$$

Here, $k_o=2\pi/\lambda$ is the free-space wavenumber, $s=k_\rho/k_o$ is the scaled radial wavenumber, n is the index of refraction of the glass substrate, t_p is the transmission coefficient of the double interface, and J_1 is the first-order cylindrical Bessel function. The integral is mainly dominated by the pole of t_p due to the surface plasmon $s\approx(\tilde{\epsilon}_m/(1+\tilde{\epsilon}_m))^{1/2}$. For distances $\rho\gg\lambda$ the field is dominated by the enhanced plasmon's E_z field. Because of the symmetry of the HE_{11} mode propagating in the core of an apertured near-field probe [20] our experiment is predominantly sensitive to $|\nabla_\perp\mathbf{E_z}|^2$. We note, however, that inside the focus, the contributions of directly transmitted rays lead to a more complex pattern containing $(\mathbf{E_x}+\mathbf{E_y})$ components of the field. For a dielectric interface, these transverse components are dominant and the probe will principally render $|(\mathbf{E_x}+\mathbf{E_y})|^2$.

To compare our experimental results with theory, we compute the intensity $I(\rho,\phi)\propto|\mathbf{E_z}(\rho,\phi)|^2$ on the surface of the metal film for different focal positions z_o without including the presence of the tip. The inset of Fig. 1(b) shows the intensity $I(\rho,\phi)$ around the focus for a focal position coinciding with the metal/air interface ($z_o=0$). The interference and the symmetry of the pattern shown in Fig. 1(b) are well reproduced in the computed $|\nabla_\perp\mathbf{E_z}|^2$ map (inset). The fringes originate from interfering SPPs with opposite wave vectors with a fringe period of 310 ± 7 nm, in agreement with the predicted SPP half-wavelength of 307 nm for $\tilde{\epsilon}_m=-18.3+i0.51$. We note that the SPP undulations are rapidly decaying in the lateral direction as shown by the cross-sectional view of the intensity. This rapid decay can be understood from the width of the dispersion relation, where the complex values of $\tilde{k}_{sp}$ are imposing a spread of SPP resonant wave vectors. The SPPs are therefore no longer excited by a single plane wave but by a collection of waves with incident angles $\Delta\theta$ centered around θ_{sp}. These waves form an effective focus for SPPs larger than the geometrical one, thus limiting the SPP excitation and interaction area.

The SPPs contribution in the intensity distribution is revealed by comparing the pattern on a bare glass substrate without the presence of the silver film under the same experimental conditions [Fig. 1(c)]. Here, the focal region is well-defined and corresponds to a diffraction-limited focal region convoluted with the aperture size and has a full width at half-maximum of $\sim$400 nm. The recorded image agrees well with the calculated map shown in the inset representing the total intensity resulting from the superposition of all the fields contained in the focus.

To understand the formation of an effective focal region for SPPs, we recorded surface plasmon intensity distributions along the same horizontal line as a function of defocus z_o to form an image representing the plane (x,z_o) as shown in Fig. 2(a). The central dashed line indicates the position ($z_o=0$) for which the geometric focus coincides with the glass/Ag interface and corresponds to the shortest spatial extension of the fringes. For $z_o<0$, the focus is below the interface and for $z_o>0$ the focus is located above the interface [see the dashed and dotted rays in Fig. 1(a)]. Figure 2(d) represents the calculated intensity $|\nabla_\perp\mathbf{E_z}|^2$ along the x-direction as a function of z_o. The evolution of the fringe pattern shown in the experimental (x,z_o) map is also found in the calculated distribution. In particular, as the focus is translated from bottom to top, the number of fringes increases. For a defocus $z_o=2$ μm the undulations are visible across the entire (x,y) transverse scan area as displayed in Fig. 2(b). This characteristic is also reproduced by the corresponding calculated in-plane map of Fig. 2(e) and confirms that the overlap area of counterpropagating SPPs, i.e., the SPP effective focus, is increasing for a positive defocus.

Let us consider now the intensity distribution of SPPs for a focus placed below the interface ($z_o<0$), i.e., in the glass substrate. Figure 2(c) shows the (x,y)

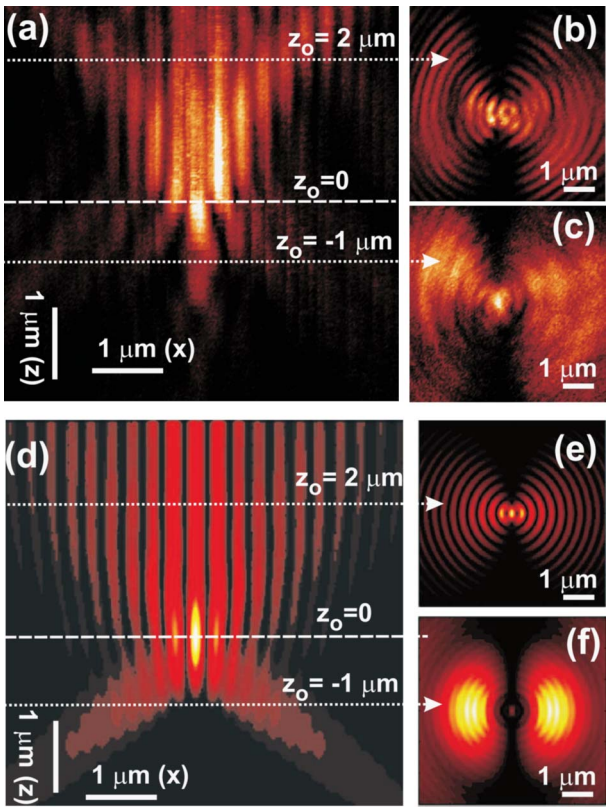

Fig. 2. (Color online) (a) (x,z_o) image showing the surface plasmon intensity along the same line for different focal positions z_o. (b), (c) (x,y)-transverse intensity maps for selected z_o. (d) Calculated $|\nabla_\perp \mathbf{E_z}|^2$ map along the (x,z_o) plane. (e), (f) Calculated (x,y) maps for $z_o=2$ μm and $z_o=-1$ μm.

transverse map for $z_o=-1$ μm. The intensity is no longer strongly modulated, which indicates that counterpropagating SPPs are not excited. Instead, the distribution resembles the two-lobe pattern characteristic of SPPs excited by a point source. The uneven intensity of the two lobes probably originates from the quality of the Gaussian beam. The two-lobe pattern is confirmed by the calculated intensity of Fig. 2(f) for the same position of the focus. Qualitatively, the absence of strongly contrasted SPP fringes can be understood on the basis that the incident rays at $\theta=\pm(\theta_{sp}\pm\Delta\theta)$ intersect *before* reaching the Ag film, thereby launching SPPs propagating in opposite directions and from separate origins [dashed line in Fig. 1(a)].

In conclusion, we find that for positive defocus ($z_o>0$) SPP-resonant incident rays launch counterpropagating surface waves, leading to an intensity map characteristic for interfering SPPs. For negative defocus incident rays launch surface waves that do not overlap and no SPP interference is observed. Our study demonstrates that tightly focused laser beams is a convenient and straightforward approach to excite SPPs and that surface plasmon self-interference can be controlled by the amount of defocus z_o. Excitation of SPPs with focused laser beams can be potentially utilized for triggering a local interaction in the next generation of active and nonlinear plasmonic devices.

Financial support for this work is provided by the Regional Council of Burgundy, the Air Force Office of Scientific Research (MURI F-49620-03-1-0379), and the Petroleum Research Foundation (PRF 42545-AC10). The work at Argonne was supported by the U.S. Department of Energy, Office of Science, Office of Basic Energy Sciences, under Contract No. DE-AC02-06CH11357.

References

1. H. Ditlbacher, A. Hohenau, D. Wagner, M. R. U. Kreibig, F. Hofer, F. R. Aussenegg, and J. R. Krenn, Phys. Rev. Lett. **95**, 257403 (2005).
2. S. I. Bozhevolnyi, V. S. Volkov, E. Devaux, and T. W. Ebbesen, Phys. Rev. Lett. **95**, 046802 (2005).
3. P. Mühlschlegel, H.-J. Eisler, O. J. F. Martin, B. Hecht, and D. W. Pohl, Science **308**, 1607 (2005).
4. A. D. McFarland and R. P. V. Duyne, Nano Lett. **3**, 1057 (2003).
5. J. B. Pendry, Phys. Rev. B **85**, 3966 (2000).
6. A. Hartschuh, E. J. Sánchez, X. S. Xie, and L. Novotny, Phys. Rev. Lett. **90**, 095503 (2003).
7. A. Bouhelier, R. Bachelot, G. Lerondel, S. Kostcheev, P. Royer, and G. P. Wiederrecht, Phys. Rev. Lett. **95**, 267405 (2005).
8. B. Hecht, H. Bielefeldt, L. Novotny, Y. Inouye, and D. W. Pohl, Phys. Rev. Lett. **77**, 1889 (1996).
9. A. Bouhelier, T. Huser, H. Tamaru, H.-J. Güntherodt, D. W. Pohl, F. I. Baida, and D. V. Labeke, Phys. Rev. B **63**, 155404 (2001).
10. S. Bozhevolnyi and F. Pudin, Phys. Rev. Lett. **78**, 2923 (1997).
11. H. Ditlbacher, J. R. Krenn, G. Schider, A. Leitner, and F. R. Aussenegg, Appl. Phys. Lett. **81**, 1762 (2002).
12. L. Yin, V. K. Vlasko-Vlasov, A. Rydh, J. Pearson, U. Welp, S.-H. Chang, S. K. Gray, G. C. Schatz, D. B. Brown, and C. W. Kimball, Appl. Phys. Lett. **85**, 467 (2004).
13. H. Gao, J. Henzie, and T. W. Odom, Nano Lett. **6**, 2104 (2005).
14. T. Rindzevicius, Y. Alaverdyan, B. Sepulveda, T. Pakizeh, M. Käll, R. Hillenbrand, J. Aizpurua, and F. J. G. de Abajo, J. Phys. Chem. C **111**, 1207 (2007).
15. A. Bouhelier and G. P. Wiederrecht, Phys. Rev. B **71**, 195406 (2005).
16. H. Kano, S. Mizuguchi, and S. Kawata, J. Opt. Soc. Am. B **15**, 1381 (1998).
17. F. D. Stefani, K. Vasilev, N. S. N. Bocchio, and M. Kreiter, Phys. Rev. Lett. **94**, 023005 (2005).
18. P. Dawson, F. de Fornel, and J.-P. Goudonnet, Phys. Rev. Lett. **72**, 2927 (1994).
19. J.-C. Weeber, J. R. Krenn, A. Dereux, B. Lamprecht, Y. Lacroute, and J. P. Goudonnet, Phys. Rev. B **64**, 045411 (2001).
20. L. Novotny and B. Hecht, *Principles of Nano-optics* (Cambridge U. Press, 2006).